JACS
JOURNAL OF THE AMERICAN CHEMICAL SOCIETY

COMMUNICATION

pubs.acs.org/JACS

A Co_4O_4 "Cubane" Water Oxidation Catalyst Inspired by Photosynthesis

Nicholas S. McCool, David M. Robinson, John E. Sheats, and G. Charles Dismukes*

Department of Chemistry and Chemical Biology, Rutgers, The State University of New Jersey, Piscataway, New Jersey 08854, United States

Supporting Information

ABSTRACT: Herein we describe the molecular Co_4O_4 cubane complex $Co_4O_4(OAc)_4(py)_4$ (**1**), which catalyzes efficient water oxidizing activity when powered by a standard photochemical oxidation source or electrochemical oxidation. The pH dependence of catalysis, the turnover frequency, and in situ monitoring of catalytic species have revealed the intrinsic capabilities of this core type. The catalytic activity of complex **1** and analogous Mn_4O_4 cubane complexes is attributed to the cubical core topology, which is analogous to that of nature's water oxidation catalyst, a cubical $CaMn_4O_5$ cluster.

A limiting technology needed for creation of solar fuels derived from renewable feedstocks is the development of efficient water oxidation catalysts made from earth-abundant materials for the oxygen-evolving half-reaction (OER) (eq 1).

$$2H_2O(l) \rightarrow O_2(g) + 4H^+(sol) + 4e^- \quad (1)$$

Important mechanistic principles of catalysis have been learned from organo-metallic compounds of various sizes from mono- to poly-nuclear clusters using noble-metals such as Ru and Ir.[1−5] However, it is essential to overcome the limiting scalability of these low-natural-abundance elements. Consequently, current research has focused on 3d transition metals for both heterogeneous[6−10] and homogeneous catalysis.[11−14]

A structural component now recognized as critical for catalysis of water oxidation is the transition-metal−oxo cubical core M_4O_4, as shown in Figure 1. This theme has been made especially clear by the studies of molecular cubanes containing the $[Mn_4O_4]^{7+}$ core[15] but has also been postulated as the catalytic core in nanocrystalline spinels Co_3O_4,[6,8] Mn_3O_4,[16] and λ-MnO_2[10] and in both solutions[17] and noncrystalline solids[9,18] of CoO_x:PO_4.

All of these cubical cores resemble the conserved catalytic core universally found in all photosynthetic enzymes that catalyze water oxidation. This core is composed of a cubical $CaMn_3O_4$ cluster that is oxo-bridged to a fourth Mn atom (Figure 1). While nature uses Mn exclusively in the photosystem II water-oxidizing complex (PSII-WOC), there are multiple examples of Co-based water oxidation catalysts, some of which outperform comparable Mn-based materials.[20,21] Only one example of a molecular cobalt catalyst has been reported and found to be amenable to detailed mechanistic studies.[20] This complex, $[Co_4(H_2O)_2(PW_9O_{34})_2]^{10-}$, consists of a planar Co_4O_{16} core sandwiched between two polyhedral $[PW_9O_{34}]$ units.

Herein we provide a second example of a structurally well-characterized homogeneous cobalt organometallic compound that catalyzes water oxidation, which is also the first example containing a cubical Co_4O_4 core. We compare its water oxidation activity to those of other catalysts to assess the generality of the bioinspired cubical topology for catalysis.[22] We also demonstrate coupling of this compound to a photosensitizer for light-induced water oxidation.

Two prior reports of molecular cobalt−oxo cubanes have been described previously: $Co_4O_4(Ac)_4(py)_4$[23] $Co_4O_4(bpy)_4(Ac)_2$.[24] An identical core type is found in both, confirming the intrinsic stability of the $[Co_4O_4]^{4+}$ core. Water oxidation by $Co_4O_4(Ac)_4(py)_4$ (**1**) has not been previously investigated. **1** has been found to catalyze oxidation of benzylic alcohols, with mechanistic studies indicating unique activity relative to Co(II) salts.[25,26]

Compound **1** was synthesized from $Co(NO_3)_2$, $Na(CH_3CO_2)$, and pyridine as described in the Supporting Information (SI). The molecular structure was confirmed by comparison of ^{1}H NMR (Figure 2a), cyclic voltammetry (CV) (Figure 3), UV−vis (Figure S1 in the SI), and MS analyses to literature data.[23] The solution structure (Figure 1a) exhibits D_{2d} point-group symmetry and is composed of a cubical $[Co_4O_4]^{4+}$ core surrounded by four bidentate acetate ligands and four monodentate pyridine ligands. The ^{1}H NMR spectrum of **1** exhibited three sets of peaks at δ 8.16, 7.69, and 7.18 for the ortho, para, and and meta ring protons of the equivalent pyridines and a singlet at δ 2.02 for the equivalent acetates (Figure 2a). A reversible one-electron redox couple at $E_{1/2}$ = 0.71 V vs Ag/AgCl was observed in acetonitrile (Figure 3), corresponding to oxidation to the formal oxidation state $[3Co^{III}, Co^{IV}]$ ($\mathbf{1}^+$) as reported previously.[23] In contrast, CV of **1** in an aqueous solution at pH 6.8 revealed a catalytic oxidative current with a prefeature indicative of the formation of an intermediate ($\mathbf{1}^+$) before water oxidation. Further electrochemical studies are in progress.

Catalytic water oxidation was monitored in solution through detection of dissolved O_2 using a thermostatted Clark-type electrode at 25 °C (Figure 4) and by gas chromatography (Figure S3). Continuous oxidation of the catalyst was provided by a standard photoexcitation system[8,27] that generates Ru^{III} upon illumination of $[Ru^{II}(bpy)_3]^{2+}$ (bpy = bipyridine) using a sacrificial acceptor (persulfate).

Photooxidation experiments were carried out under constant solution conditions (0.5 mM $[Ru(bpy)_3]^{2+}$ and 35 mM $Na_2S_2O_8$). Control experiments were performed in which each

Received: April 27, 2011
Published: July 08, 2011

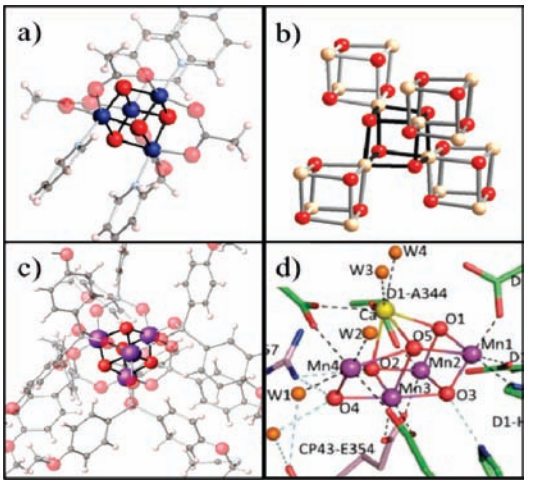

Figure 1. Crystal structures of active water oxidation catalysts: (a) $Co_4O_4(Ac)_4(py)_4$ (**1**); (b) spinel λ-MnO_2 subunit structure; (c) $Mn_4O_4L_6$ catalyst core; (d) PSII-WOC[19].

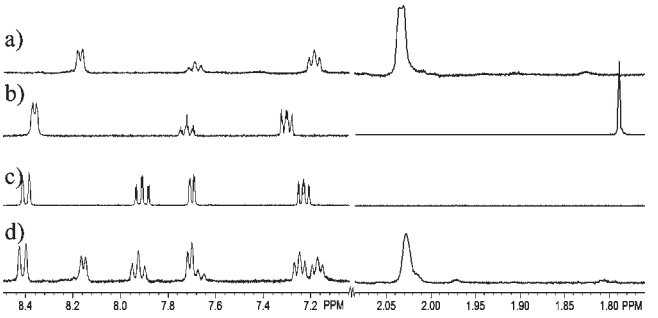

Figure 2. ^{1}H NMR spectra in D_2O of (a) **1** (1 mM), (b) pyridine (4 mM) and sodium acetate (4 mM), (c) $Ru(bpy)_3^{2+}$ (1 mM), and (d) a mixture of **1** (1 mM) and $Ru(bpy)_3^{2+}$ (1 mM).

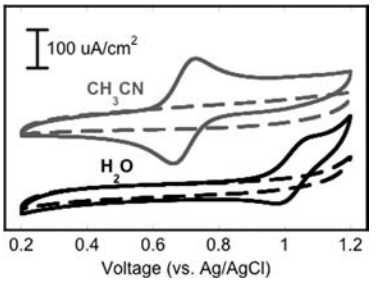

Figure 3. Cyclic voltammograms of 1 mM **1** (solid lines) and a bare glassy carbon electrode (dashed lines) in (gray) 0.1 M tetrabutylammonium perchlorate in CH_3CN and (black) 0.1 M Na_2SO_4 in H_2O.

individual component of the system was removed {light (Figure S2), $S_2O_8^{2-}$, $[Ru(bpy)_3]^{2+}$, and **1**}; they yielded no O_2 production, confirming the necessity of all components for light-driven O_2 production (Figure S7). The specific turnover frequency (TOF) of the catalyst was observed to be 0.02 mol O_2 (mol of **1**)$^{-1}$ s^{-1} at room temperature with 50 μM catalyst (see Table 1). Initial-rate experiments revealed a complex kinetic dependence on the concentrations of the components of the photooxidant system and were not pursued further. Headspace

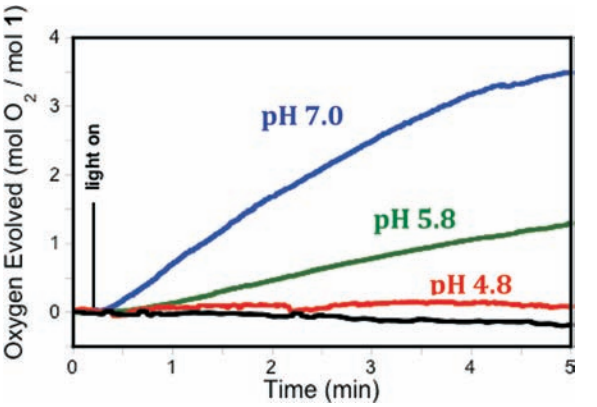

Figure 4. Clark electrode data showing O_2 concentration in solution before and after the onset of illumination of [**1**] (0.33 mM) in the presence of 0.5 mM $[Ru(bpy)_3]^{2+}$ and 35 mM $Na_2S_2O_8$ in (blue) HCO_3^- buffer at pH 7.0, (green) SiF_6^{2-} buffer at pH 5.8, and (red) SiF_6^{2-} buffer at pH 4.8. The black curve shows data without catalyst at pH 5.8. Controls at all pHs exhibited no O_2 production without catalyst.

O_2 yields were monitored using gas chromatography, and turnover numbers (TONs) were determined (Figure S3). Control experiments on solutions separately lacking one of the components produced baseline oxygen peaks indistinguishable from the purge control. The TON determined after 60 min of illumination was 40 $\pm$ 2 (see Table 1). The time interval for the TON was deliberately limited to 1 h because of photodecomposition of the $Ru(bpy)_3^{2+}$ complex, as described below.

In order to identify the species present during catalytic turnover, we monitored all components of the complete photocatalytic system using ^{1}H NMR spectroscopy. Solutions were prepared by mixing **1** with free pyridine, free acetate, or $Ru(bpy)_3^{2+}$, which established that the ^{1}H NMR peaks of the ligated pyridines and acetates on **1** are readily distinguishable from those of the corresponding unbound molecules and the bipyridine ligands of $Ru(bpy)_3^{2+}$ (Figure 2). Dissolved and headspace-accumulated oxygen production were monitored in a D_2O buffer in conjunction with ^{1}H NMR analysis. ^{1}H NMR spectra of the reaction solutions were taken before and after illumination, indicating the quantitative yield of **1** before and after oxygen production by observation of both the ligated pyridine and acetate peaks. Quantitative analysis of the ^{1}H NMR peaks using an internal standard (see the SI) indicated <5% photodecomposition of **1** in contrast to 65% photodecomposition of $Ru(bpy)_3^{2+}$ after 10 min of illumination (Figure 5). Thus, ^{1}H NMR analysis over >5 turnovers showed that **1** remains intact and is the catalytic species responsible for water oxidation. The substantial decay of the bipyridine ligand peaks of $Ru(bpy)_3^{2+}$ over the same time interval indicates that this photodecomposition limits the catalyst TON measurements.

Possible photodecomposition byproducts of **1** include aqueous Co species, acetate, and pyridine. Aqueous Co(II) has been shown previously to be a precursor to the formation of a water oxidation catalyst upon illumination.[17] Consequently, we investigated the catalytic activities of both **1** and aqueous Co(II) to establish the source of the activity attributed to **1**. The absence of Co(II) impurities in **1** was established by ^{1}H NMR analysis (Figure 2 and Figure S6), which is very sensitive for the detection of all components including Co(II) because of paramagnetic line broadening effects. With a maximum of 5% decomposition of **1**

dx.doi.org/10.1021/ja203877y |J. Am. Chem. Soc. 2011, 133, 11446–11449

Table 1. Comparison of the Catalysis Capabilities of Various Molecular Water Oxidation Catalysts

catalyst material	TOF (s^{-1})	TON	oxidant
$Co_4O_4(py)_4(Ac)_4$	2.0×10^{-2}	>40	$Ru^{III}(bpy)_3^{3+}$
$Mn_4O_4(MeOPh_2PO_2)$/Nafion[a]	2.4×10^{-4}	>1000	1.2 V
$[Co_4(H_2O)_2(PW_9O_{34})_2]^{10-}$ [b]	5×10^{0}	>1000	$Ru^{III}(bpy)_3^{3+}$
$[(tpy)(H_2O)Mn(O)_2Mn(H_2O)(tpy)]^{3+}$ [c]	6.7×10^{-1}	>50	HSO_5^-
PSII-WOC	5×10^{2}	10^7	Tyr radical

[a] Data from ref 11. [b] Data from ref 20. [c] Data from ref 13.

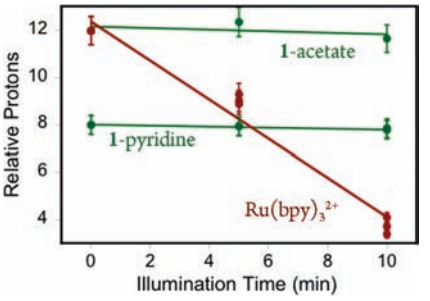

Figure 5. Relative ^{1}H NMR integration intensities (normalized to an internal standard) of the peaks for the bound acetates in **1** (upper green), the bound pyridines in **1** (lower green), and the bipyridines in $[Ru(bpy)_3]^{2+}$ (red) following 5 and 10 min of illumination (2 mW/cm^2). The experiments were done in triplicate. The reaction conditions were 0.5 mM **1**, 0.5 mM $[Ru(bpy)_3]^{2+}$, and 35 mM $Na_2S_2O_8$.

into aqueous Co species (Figure 5), catalytic experiments with concentrations of Co(II) at 5% of the observably active concentrations of **1** were incapable of producing measurable O_2 evolution. If it is assumed that decomposition of **1** yields an active competing catalyst, the possible decomposition products do not produce O_2 yields in competitive quantities.

Additional experiments demonstrated distinct kinetics of oxygen evolution activity for **1** and aqueous Co(II) (Figure 6). Increasing the concentration of Co(II) had a significant effect on delaying the onset time for O_2; the delay time following illumination rapidly increased from 10 s (minimum) to 180 s. A precipitate rapidly formed at increasing concentrations, indicative of an inactivating side reaction as reported previously.[17] In contrast, **1** exhibited no lag in catalysis following illumination. The minor increase in the lag time for **1** (Figure 6) can be attributed to an decreasing oxidant:catalyst ratio, requiring more time for generation of sufficient oxidized $Ru(bpy)_3^{3+}$ and possible sequential oxidation steps per catalyst, as shown by CV (Figure 3).

Table 1 reveals that **1** compares favorably with several other homogeneous water oxidation catalysts based on abundant 3d transition metals. TOF comparisons are limited because of the varied oxidant systems used. However, the highest TOFs using the cationic $Ru^{III}(bpy)_3^{3+}$ photooxidant system occur for anionic catalysts. This is not surprising for this homogeneous system and reveals that diffusion or binding of these components is rate-limiting. Our future work will examine the electrocatalytic oxidation of water by **1**. The natural photosynthetic center has a TOF that is several hundred-fold higher and operates over a much wider pH range than the model systems.

The metal−oxo cubical core is a unifying structural feature observed in a wide range of water oxidation catalysts made from

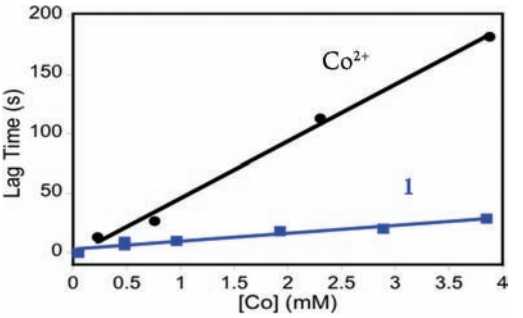

Figure 6. Time elapsed following illumination in the presence of 0.5 mM $[Ru(bpy)_3]^{2+}$ and 35 mM $Na_2S_2O_8$ before the onset of oxygen production normalized to cobalt atoms as measured using a Clark electrode for Co^{2+} (black) and **1** (blue).

3d transtion metals, including **1**, the PSII-WOC, the molecular Mn_4O_4 cubanes, and the modified spinel-phase complexes (Figure 1). A proposed mechanism for O_2 evolution from the PSII-WOC has postulated that this core type is essential for formation of the peroxo intermediate from two μ_3-O bridges as a precursor to O_2 release.[28] A very similar mechanism has been proposed for the Mn_4O_4 cubane-core compounds[22] and has recently been confirmed by density functional theory calculations.[29] These diverse examples of metal−oxo cubical core types provide stronger evidence that this topology is the critical structural feature responsible for the water oxidation activity in both the natural photosynthetic enzyme and bioinspired mimics.

■ ASSOCIATED CONTENT

Supporting Information. Figures S1−S7, synthesis of **1**, preparation of photooxidant system, light source information, experimental details for the oxygen evolution procedure, and ^{1}H NMR spectra and analysis. This material is available free of charge via the Internet at http://pubs.acs.org.

■ AUTHOR INFORMATION

Corresponding Author
dismukes@rci.rutgers.edu

■ ACKNOWLEDGMENT

We thank Clyde Cady, Yong-Bok Go, and Nick Bennette for discussions. This work was supported by an NSF Predoctoral Fellowship (D.M.R.), AFOSR Grant FA9550-05-1-0365, and Rutgers University.

■ REFERENCES

(1) McDaniel, N. D.; Coughlin, F. J.; Tinker, L. L.; Bernhard, S. *J. Am. Chem. Soc.* **2008**, *130*, 210.
(2) Youngblood, W. J.; Lee, S.-H. A.; Kobayashi, Y.; Hernandez-Pagan, E. A.; Hoertz, P. G.; Moore, T. A.; Moore, A. L.; Gust, D.; Mallouk, T. E. *J. Am. Chem. Soc.* **2009**, *131*, 926.
(3) Sens, C.; Romero, I.; Rodríguez, M.; Llobet, A.; Parella, T.; Benet-Buchholz, J. *J. Am. Chem. Soc.* **2004**, *126*, 7798.
(4) Nagoshi, K.; Yamashita, S.; Yagi, M.; Kaneko, M. *J. Mol. Catal. A: Chem.* **1999**, *144*, 71.
(5) Hull, J. F.; Balcells, D.; Blakemore, J. D.; Incarvito, C. D.; Eisenstein, O.; Brudvig, G. W.; Crabtree, R. H. *J. Am. Chem. Soc.* **2009**, *131*, 8730.

(6) Esswein, A. J.; McMurdo, M. J.; Ross, P. N.; Bell, A. T.; Tilley, T. D. *J. Phys. Chem. C* **2009**, *113*, 15068.
(7) Harriman, A.; Pickering, I. J.; Thomas, J. M.; Christensen, P. A. *J. Chem. Soc., Faraday Trans. 1* **1988**, *84*, 2795.
(8) Jiao, F.; Frei, H. *Angew. Chem., Int. Ed.* **2009**, *48*, 1841.
(9) Kanan, M. W.; Yano, J.; Surendranath, Y.; Dincă, M.; Yachandra, V. K.; Nocera, D. G. *J. Am. Chem. Soc.* **2010**, *132*, 13692.
(10) Robinson, D. M.; Go, Y. B.; Greenblatt, M.; Dismukes, G. C. *J. Am. Chem. Soc.* **2010**, *132*, 11467.
(11) Brimblecombe, R.; Kolling, D. R. J.; Bond, A. M.; Dismukes, G. C.; Spiccia, L.; Swiegers, G. F. *Inorg. Chem.* **2009**, *48*, 7269.
(12) Kurz, P.; Berggren, G.; Anderlund, M. F.; Styring, S. *Dalton Trans.* **2007**, 4258.
(13) Limburg, J.; Vrettos, J. S.; Chen, H. Y.; de Paula, J. C.; Crabtree, R. H.; Brudvig, G. W. *J. Am. Chem. Soc.* **2001**, *123*, 423.
(14) Ellis, W. C.; McDaniel, N. D.; Bernhard, S.; Collins, T. J. *J. Am. Chem. Soc.* **2010**, *132*, 10990.
(15) Brimblecombe, R.; Koo, A.; Dismukes, G. C.; Swiegers, G. F.; Spiccia, L. *J. Am. Chem. Soc.* **2010**, *132*, 2892.
(16) Jiao, F.; Frei, H. *Chem. Commun.* **2010**, *46*, 2920.
(17) Brunschwig, B. S.; Chou, M. H.; Creutz, C.; Ghosh, P.; Sutin, N. *J. Am. Chem. Soc.* **1983**, *105*, 4832.
(18) Kanan, M. W.; Nocera, D. G. *Science* **2008**, *321*, 1072.
(19) Umena, Y.; Kawakami, K.; Shen, J.-R.; Kamiya, N. *Nature* **2011**, *473*, 55.
(20) Yin, Q.; Tan, J. M.; Besson, C.; Geletii, Y. V.; Musaev, D. G.; Kuznetsov, A. E.; Luo, Z.; Hardcastle, K. I.; Hill, C. L. *Science* **2010**, *328*, 342.
(21) Jiao, F.; Frei, H. *Energy Environ. Sci.* **2010**, *3*, 1018.
(22) Dismukes, G. C.; Brimblecombe, R.; Felton, G. A. N.; Pryadun, R. S.; Sheats, J. E.; Spiccia, L. *Acc. Chem. Res.* **2009**, *42*, 1935.
(23) Chakrabarty, R.; Bora, S. J.; Das, B. K. *Inorg. Chem.* **2007**, *46*, 9450.
(24) Dimitrou, K.; Folting, K.; Streib, W. E.; Christou, G. *J. Am. Chem. Soc.* **1993**, *115*, 6432.
(25) Chakrabarty, R.; Sarmah, P.; Saha, B.; Chakravorty, S.; Das, B. K. *Inorg. Chem.* **2009**, *48*, 6371.
(26) Sarmah, P.; Chakrabarty, R.; Phukan, P.; Das, B. K. *J. Mol. Catal. A: Chem.* **2007**, *268*, 36.
(27) Morris, N. D.; Suzuki, M.; Mallouk, T. E. *J. Phys. Chem. A* **2004**, *108*, 9115.
(28) Dasgupta, J.; van Willigen, R. T.; Dismukes, G. C. *Phys. Chem. Chem. Phys.* **2004**, *6*, 4793.
(29) Kuznetsov, A. E.; Geletii, Y. V.; Hill, C. L.; Musaev, D. G. *J. Phys. Chem. A* **2010**, *114*, 11417.